Title: Body anatomical UV protection predicted by shade structures: a modeling study

Authors: Religi A, Backes C, Moccozet L, Vuilleumier L, Vernez D, Bulliard J

Journal: Photochemistry and Photobiology

Year: 2018

Issue: 94

Volume: 6

Pages: 1289-1296

DOI: 10.1111/php.12949

Article type : Research Article

Body Anatomical UV Protection Predicted by Shade Structures: a Modeling Study

A. Religi[1*], C. Backes[2,3], L. Moccozet[1], L. Vuilleumier[4], D. Vernez[2], J-L. Bulliard[3]

[1] Institute of Information Service Science, University of Geneva, Geneva, Switzerland

[2] Institute for Work and Health, University of Lausanne and Geneva, Lausanne, Switzerland

[3] University Institute of Social and Preventive Medicine, Centre Hospitalier Universitaire Vaudois (CHUV) and University of Lausanne, Lausanne, Switzerland

[4] Federal Office of Meteorology and Climatology, MeteoSwiss, Payerne, Switzerland

*Corresponding author e-mail: Arianna.Religi@unige.ch (Arianna Religi)

ABSTRACT

Shade is an important means of protection against harmful effects of sun ultraviolet (UV) exposure, but not all shades are identically protective. UV rays scattered by the atmosphere and surroundings can reach the skin indirectly. In order to evaluate the relative contribution of the direct, diffuse and reflected radiation in UV protection provided by different sizes of shade structure, we used SimUVEx

This article has been accepted for publication and undergone full peer review but has not been through the copyediting, typesetting, pagination and proofreading process, which may lead to differences between this version and the Version of Record. Please cite this article as doi: 10.1111/php.12949

v2, a numeric tool based on 3D graphic techniques and ambient ground UV irradiance. The relative UV exposure reduction was expressed by the predictive protection factor (PPF). Shade structures were found to predominantly reduce exposure from direct radiation (from 97.1% to 99.9% for the upper body areas such as the head and the neck), with greater protection from larger shade structures and structures closer above the subject. Legs were the least protected anatomical zone from any shade structure above the subject with PPF ranging from 18.5% to 68.1%. Throughout the day, except for lower solar zenith angles (SZA), small and high shade structures provide the lowest protection (between 20% and 50%), while small and low shade structure show PPF between 35% and 65% and large and high shade structures reach PPF higher than 60%.

INTRODUCTION

Shade is an important sun protection means, but not all shades are identically protective from UV radiation. While the direct UV component is incident on a particular spot, having travelled a straight path from the sun, the diffuse and reflected components come from all directions since they are scattered by clouds and other elements in the atmosphere, or bounced back from UV reflective surfaces (e.g., sand, snow, water). Diffuse radiation provides a very large contribution to solar UV exposure on non-horizontal surfaces (such as most of the human anatomical zones), explaining about 80% of the cumulative annual exposure dose on human body (1). Thus, even if shade reduces direct UV exposure, diffuse UV radiation can reach the shaded skin, entering through the side openings of the shade structure, leaving people in the shade exposed to indirect UV radiation. The size, the shape, the height and the fabric of the shade structure along with the position of the occupant can influence the level of UV exposure of anatomical zones. Moreover, the shade projected by

the structure changes over the day and when the sun is low (i.e., for higher SZA), the shade protection may not be below the shade structure (2). Previous works have shown that scattered UV levels under shade structures are sufficiently important to cause sun related damage (2-4). Dosimetric measurements show significant decreases in exposure under shade structures up to 65% for summer and 57% for winter (5). Nonetheless, even if dosimetric studies are valid instruments to quantify the amount of individual UV exposure, measurements are strongly related to their specific location, and the orientation of the dosimeter. In most cases, they measure the total radiation received, without differentiating the relative contribution of each UV component.

Very few studies have reported measurements for global (direct and diffuse) radiation combining radiometer measurements and sky view factor models (6, 7). Furthermore, the anatomical geometry of individuals is highly heterogeneous and the incident intensity on tilted planes can exceed that on horizontal surfaces in some specific topographical conditions (8-10), and nearly doubles on vertical planes (11). In order to quantify anatomical site-specific UV exposure with respect to the direct, diffuse and reflected components, we developed SimUVEx v2 (12, 13), a numerical tool based on 3D graphic techniques and human modeling to estimate the exposure of a 3D virtual mannequin. Human modeling that combines technology with science is widely implemented in various fields such as medical treatment (14, 15), surgery (16), ergonomics (17, 18), film and television (19), and sports (20, 21). Although several studies have addressed the human body exposure to UV (22, 24), to the best of our knowledge, very limited efforts have been brought to the application of human modeling and 3D computer graphics for estimating and visualizing UV exposure (25). The aims of this research are to predict the UV exposure reduction provided by shade structures and evaluate how the reduction is influenced by diffuse and reflected radiation.

MATERIALS AND METHODS

Modelling tool. SimUVEx v2 is a numeric tool that uses 3D graphics techniques to estimate the exposure of a virtual mannequin on the basis of postural information, continuous ambient radiation datasets and shade factors (headgear, shade structures, sunglasses, etc.). The virtual mannequin is depicted as a 3D mesh of connected triangles, whose size density depends on the resolution. The irradiance data contains information about the sun position (defined by azimuth and zenith angle) and measured direct, diffuse and reflected radiation for every minute of the day. Each triangle of the mannequin receives a certain quantity of solar energy depending on the body surface orientation to the sun and the shadows from other anatomical zones or eventual shading structure. The direct component is described as a parallel source of irradiation varying in intensity with time and in direction with the position of the sun, whereas the diffuse and the reflected components are considered hemi-spherical isotropic sources with intensities varying as a function of time. To account for anisotropy, the diffuse radiation is assumed to decrease linearly from an elevation angle of 25° to the horizontal layer. This nearly isotropic approximation introduces uncertainties because it is not completely valid in clear-sky situations or when there is broken cloud coverage. The result is an overestimation of real exposure by a maximum of 4%-6% (26). The total irradiation received from a single triangle is expressed in ^{2} as a combination of exposure from the three components. A 3D visualization of UV exposure on the mannequin is provided to enhance understanding of the results. The principles, the performance and the validation of SimUVEx have been described previously (12, 13, 27, 28).

Ground irradiance data. Erythemally weighted direct, diffuse and reflected UV irradiances are measured at the MeteoSwiss Payerne Station (46.815°N, 6.944°E, altitude 491 m) using SolarLight SL 501A broadband radiometers with filters mimicking the erythemal response. Radiometers measuring direct and diffuse components are mounted on sun-following tracker; the

one measuring the reflected radiation is turned upside down. Daily quality control procedures are performed on the irradiance data using plausibility criteria on the individual data components as well as comparing the global UV irradiance to the sum of the direct and diffuse components. In addition, the UV radiometers are replaced every year with radiometers that underwent a calibration check. The calibration check involves a 4-months comparison at Payerne with three reference instruments of the same type (SL501A) that are regularly calibrated (at least one of the reference instrument triad is calibrated every year) at the UV section of the World Radiation Center at Davos (PMOD/WRC). The 4-months comparison occurs from March to June, when the ozone column is most variable. The raw signals of the tested instruments and the reference triad instruments are compared to first derive an overall calibration factor valid for a total ozone column of 300 DU and a solar zenith angle of 45°. Then it is checked that the ozone and solar zenith angle dependence of the calibration factor for the tested instrument can be smoothly derived (with a two-dimensional third-order polynomial fit) from the ozone and solar zenith angle dependence of the reference triad. This allows deriving both an overall calibration factor and an ozone-solar zenith angle matrix that is applied to the tested instrument raw signals for deriving UV erythemal irradiance data for the 4-months comparison. For each tested radiometer, if more than 5% of the irradiance data disagree by more than 5% from the mean of the corresponding irradiance of the reference triad, the tested radiometer is rejected and not used in the network.

Implementation. The virtual mannequin used in this article represents an adult male 1.73 m high in the seated south facing position, placed at the center of three different shading protective structures of a square shape. The structures were chosen so that a range of differently sized shade structures could be investigated. Details of the structures are as follows:

- Shade structure 1 (small/low shade structure): the first shade structure is 1 m wide and 40 cm above the top of the head of the seated mannequin;

- Shade structure 2 (small/high shade structure): the second shade structure is 1 m wide and 80 cm above the top of the head of the seated mannequin;

- Shade structure 3 (large/high shade structure): the third shade structure is 2 m wide and 80 cm above the top of the head of the seated mannequin.

Each anatomical zone is characterized by a different color and the body regions are constituted of 7 zones (head, neck, leg right/left, arm right/left, trunk) further divided in subregions.

Simulations were run for a summer cloudless day (17/07/2014) for a seated posture in static orientation to the sun without protective clothing. Two exposure scenarios were considered: at midday (12PM - 2PM, with a minimum SZA value of 25.65° at solar noon) and for a full day (8AM - 5PM). The shade structure was designed as an opaque objet providing full shielding against UV radiation. This allowed us to investigate the protection from the shade structure, without taking into account arbitrary fabric sun protection factors. The overall relative UV protection provided by the shade was expressed in percentage as a predictive protective factor (PPF), calculated according to the following equation:

$$PPF\ [\%] = \frac{UV_{withoutprotection} - UV_{withprotection}}{UV_{withoutprotection}} \times 100 \qquad (1)$$

where $UV_{withprotection}$ is the erythemal UV in the shade for a specific anatomical zone and $UV_{withoutprotection}$ is the erythemal UV for the same zone without shade. The greater the PPF, the higher the relative UV exposure reduction of the shade structure. When the PPF is equal to zero, the exposure does not change with or without protection (unprotected zone).

RESULTS

Total erythemal UV exposures received by the main anatomical zones with and without the three shade structures are represented in Fig. 1 for changing SZA during a full clear sky day.

The UV exposures per minute show a general decrease for all anatomical zones as the SZA increases. For all the unprotected situations, values range from zero, when the sun is , to 5 J/m^{2}min when the sun is at its highest elevation (SZA = 25^o). Each shade structure reveals different peak periods where the exposure increases. These periods do not arise necessary when the sun is at its highest elevation (minimum SZA) and depend on the position and size of the shadow below the shade structure. Generally they occur when the sun is lower (higher SZA) and the radiation can get in sideways. That means that each anatomical zone is shaded at different SZA depending on the position of the sun and the orientation of the considered anatomical zone during the day. For example, the head shows a peak period at around 45°-60° for the small and low shade structure, at 40°-50° for the small and high shade structure and at 40°-55° for the large and high shade structure. Overall, the head and the trunk were the most efficiently protected anatomical zones by an overhanging shading structure iting the total UV exposures below 2.5 J/m^{2}min. The situation is different for the arms and legs due to the position and the size of the shadow under the shade structure. Noteworthy, structures 1 and 2 provide a similar protection for the legs since, in those cases, they are not directly covered. The largest shade structure represented as a purple line in Fig. 1 is the most protective one, while the smallest shade structure is more protective when located closer above the subject (far 40 cm vs 80 cm). The higher and smaller the tent, the more likely the shade did not protect all anatomical zones at any time during the day.

The relative amount of UV protection provided by each shade structure, expressed as PPF, are displayed in Fig. 2 as function of time. Again, the shade structure 2 provides the lowest values, especially for the peripheral areas such as the leg (PPF below 20%) and the arm (PPF below 30%). For each shade structure, values of PPF were quite constant for every hour of the day, except in early morning (before 10AM) where the above-mentioned peak periods occur. Except for those periods, PPF range between 35 and 65% for shade structure 1, between 20 and 50% for shade structure 2 and reach values above 60% for shade structure 3.

The erythemal UV levels for each radiation component during a full summer day are displayed in Fig. 3 for the three shade structures for the head and the trunk, i.e., the anatomical zones that received the lowest exposure estimated when protected. Overall, the main effect of shade structure is to decrease the direct radiation, while the amount of diffuse and reflected UV present beneath a shade structure are proportionate to the amount of open sky visible from the shade. For the head, the reduction of the direct exposure ranges from a ximum value of about 2 J/m^{2}min to zero for all the situations, for the trunk the reduction is always complete. For the shade structure 2, it ranges from 1.8 J/m^{2}min to about 0.5 ^{2}min. The largest shade structure is the most protective, while direct radiation for both arms and legs for shade structure 1 and 2 does not decrease appreciably since these anatomical zones are not completely located in the shade. Hence, larger shaded areas provide more sun protection for more anatomical zones than smaller shade structures only if the shade structure is sufficiently large.

The PPFs provided by the three structures from 12PM to 2PM are shown in Table 1 by anatomical zone and UV radiation component (see Table S1 in the Supporting Information for a complete overview of each anatomical subregion). The related 3D rendering is shown in Fig. 4.

PPFs were highest for direct exposure on the upper body areas, such as the head and the neck, varying between 97.1% to 100% across the shade structures. There is an asymmetry with respect to arm right and left, due to the fact that the chosen time period is not centered on solar noon, as shown in Fig. 4.

In general, having chosen a two-hour exposure after solar noon, when the sun is in the western half of the sky, the right arm of the mannequin is more exposed than the left one for shade structures 1 and 2, reaching PPF of 20.5% and 55.8%, respectively, in the case of lowest protection (shade structure 2). The situation was more homogenous for the third structure where both sides were identically protected. The trunk was well protected by the shade structure 1 and 3 (PPF of 83.8% and 99.9%, respectively), but the protection was remarkably reduced for the small and high shade structure (PPF=60.5%). Results show a clear gradient in exposure from top to bottom, for each of the three situations (see Table S1). The legs were the most exposed as they are furthest away from the source of shade in the shade structures 1 and 2, with PPF ranging from 3.9% to 4.7%. Lower back and feet were the highest exposed zones of the lower limbs. Diffuse exposure was moderately decreased by shade provision. Higher PPF values (up to about 56%) were only found for the head due to the decreased amount of sky view. Reflected exposure did not vary remarkably since the experiment used measurements collected over the grass, but this quantity is mainly dependent on the surrounding surfaces. For instance, snow can reflect as much as 80% of UV radiation, dry beach sand about 15% and sea foam about 25% (29).

DISCUSSION

The amount of UV protection provided by a structure depends on various elements such as the size of the structure, its distance from the subject, its orientation to the sun, the solar position, the degree of cloud cover and the reflection of the surface. UV exposures estimated in this research illustrate the relative contribution of the components of UV radiation for three shade structures differing in size and height above the subject. Although shade structures attenuated the variability in UV exposure across the whole body, our results show that in many situations open shade provide inadequate sun protection since it is susceptible to intrusion by scattered and reflected UV radiation. Large decreases in UV exposure were found for the direct radiation from 97.1% to 99.9% for upper body areas such as the head and the neck. On the contrary, the amount of diffuse radiation that hits the skin depended on the amount of open sky visible from each anatomical zone in the shade. The results pointed to the importance of the exposure to diffuse UV radiation that decreased far less than the exposure to direct radiation in presence of shade structures, and tended to never approach zero. Indeed, the UV exposures in the shade shown in Table 1 ranged from approximately 140 to 230 J/m^2, or roughly 1 MED. This shows that a subject wearing a bathing suit with no further means of sun protection under a sun umbrella would be exposed in 2 hours (12 PM- 2PM), in summer, to sufficient diffuse UV exposure to induce a sunburn (30). It should be emphasized that irradiance measurements for an ordinary surface (i.e. grass) were used for this study. Except for the sand and the snow, the albedo of the Earth surface is nearly dark in the UV part of the spectrum with values typically between 3 and 5% (31) so that a very small component of the UV radiation is reflected upwards and consequently reflected radiation has negligible influence on the results presented here.

Our results support that not all shade structures provide adequate protection against damaging UV radiation for changing SZA and that effective sun protection requires the combination of several means of protection. The most effective shading is the one that cuts as much as possible the visible sky from the different body parts, namely the largest and highest shade structure.

However, its effectiveness depends on the sun position and the considered skin zone. For example, the lower legs and the feet were the most exposed zones of the lower limbs for any shade structure. These areas are particularly susceptible to sunburn since they also tend to be forgotten when applying sunscreen (32, 33).

The results presented in our research are in line with previous studies on solar protections based on dosimeters placed vertically (34) or horizontally at the center of a shade structure (2, 3, 5, 35), or worn at the wrist (36), or sky obstruction geometrical model (7). Previous studies generally measure the total UV radiation without quantifying diffuse and reflected radiation separately and without taking into account non-horizontal surfaces which are essential for a correct evaluation of UV exposure on anatomical zones. Indeed, shade structures can provide reasonable protection on horizontal surface, but do protect poorly on vertical surfaces (34). The large variability of the shade over the whole body (see Table S1), shows that provision of only a single protection value, regardless of the anatomical region, is inaccurate. Poor protections were found at larger SZA (lower sun) while a better protection was found at lower SZA, i.e., around midday, whether in our modelling study or in dosimetric studies (2, 5, 34). In (5) UV radiation decreases by up to 87% in the first case and up to 30% in the second case. This observation is confirmed in our research by the shape of direct radiation (blue line) in Fig. 3.

To our knowledge, very limited efforts have been brought to the application of human modeling and 3D computer graphics for estimating UV exposure (25, 37-39) and none of them refers to sun protection specifically. In this study, all results were obtained with SimUVEx, an inexpensive tool that estimates individual UV exposure distribution over the human body. SimUVEx has been validated by CIE erythemally weighted Spore film dosimeters (BioSense, Bornheim, Germany) in real on- field measurements (27) which includes measurements of total irradiance. The dosimeters used for the model validation were positioned on an articulated foam mannequin for individual exposure measurements. The validation took into account shade from other body parts and the orientation of

all surfaces. The seated posture of an adult subject located under the center of the shade structure was chosen since it represents one of the most typical positions taken under a shade structure (i.e., a sun umbrella or a tent). Production of the same analysis for other postures, morphologies (female, child, overweight person) or sun orientation is possible with SimUVEx (12) as well as the application of a simple sun reduction factor, such as the SPF, in order to investigate precisely the protection of any shade structure, based for instance on its fabric, rather than assuming an opaque object blocking 100% of direct UV radiation. The outcomes from the three shade structures can be generalized to other structures of similar size, solar orientation, sky view fractions and no surrounding surfaces of high reflectivity. The same analysis was run for a cloudless spring day (09/04/2014), i.e. when it could be common to use a shade structure to protect oneselves from the sun. Results (not shown) were also linked to the geometry of the protections and overall similar to those discussed in this work.

Skin cancer prevention messages should focus more on the important but still largely underestimated contribution of indirect UV radiation in the total UV exposure received (31). Prevention strategies should also sensitize the general public to the potential limitations of a single means of protection, such as shade, in the effectiveness of sun protection. A tool like SimUVEx can contribute to improve our understanding of exposure patterns and identify some potential shortcomings in current sun protection recommendations. It could be used, for example, to design shade structures with the purpose to exclude as much sky radiation as possible, setting different heights or sizes, responding to the need for appropriate creation of structural shade (33). Future developments could consider more complex shade situations such as trees and natural vegetation, where movement of canopy leaves and branches could lead to large fluctuations in UV exposure, or combination of different shade structures, where the sky view can be critically reduced. The degree of protection would depend on the density and location of the closest structures.

ACKNOWLEDGEMENTS: This work is supported by the Swiss National Science Foundation (grant no. CR23I3 152803) with the research project PuRSUE (PRedict Solar Uv Exposure, full title: Ground UV irradiance and 3D rendering techniques to predict anatomical solar UV exposure in Skin cancer research).

SUPPLORTING INFORMATION

Additional Supporting Information is available in the online version of this article:

Table S1. Predictive protection factor (PPF, in %) of three shade structures for main anatomical regions between 12 PM and 2 PM.

REFERENCES

1. Vernez, D., A. Milon, L. Vuilleumier and J. L. Bulliard (2012) Anatomical exposure patterns of skin to sunlight: relative contributions of direct, diffuse and reflected ultraviolet radiation. British Journal of Dermatology, 167(2), 383-390.

2. Turnbull, D. J., A. V. Parisi, and J. Sabburg (2003) Scattered UV Beneath Public Shade Structures During Winter. Photochemistry and photobiology, 78(2), 180-183.

3. Turnbull, D. J. and A. V. Parisi, (2003) Spectral UV in public shade settings. Journal of Photochemistry and Photobiology B: Biology, 69(1), 13-19.

4. Toomey, S. J., H. P. Gies, and C. R.Roy (1995) UVR protection offered by shadecloths and polycarbonates. Radiation Protection in Australia, 13(2).

5. Turnbull, D. J., and A. V. Parisi (2005) Increasing the ultraviolet protection provided by shade structures. Journal of Photochemistry and Photobiology B: Biology, 78(1), 61-67.

6. Kudish, A. I., M. Harari, and E. G. Evseev (2011) The solar ultraviolet B radiation protection provided by shading devices with regard to its diffuse component. Photodermatology, photoimmunology & photomedicine, 27(5), 236-244.

7. Utrillas, M. P., J.A. Martínez-Lozano and M. Nunez (2010) Ultraviolet radiation protection by a beach umbrella. Photochemistry and photobiology, 86(2), 449-456.

8. Weihs, P. (2002) Influence of ground reflectivity and topography on erythemal UV radiation on inclined planes. International journal of biometeorology 46.2 95-104.

9. Siani, A. M., Casale, G. R., Diemoz, H., Agnesod, G., Kimlin, M. G., Lang, C. A., and Colosimo, A. (2008) Personal UV exposure in high albedo alpine sites. Atmospheric Chemistry and Physics, 8(14), 3749-3760.

10. Casale, G. R., Siani, A. M., Diémoz, H., Agnesod, G., Parisi, A. V., and Colosimo, A. (2015) Extreme UV index and solar exposures at Plateau Rosà (3500 m asl) in Valle d'Aosta Region, Italy. Science of the Total Environment, 512, 622-630.

11. Serrano, D., M. J. Marin, M.P. Utrillas, F. Tena and J.A. Martinez-Lozano (2012) Modelling of the UV Index on vertical and 40° tilted planes for different orientations. Photochemical and Photobiological Sciences, 11(2), 333-344.

12. Religi, A., L. Moccozet, M. Farahmand, L. Vuilleumier, D. Vernez, A. Milon, J-L Bulliard and C. Backes (2016) Simuvex v2: a numeric model to predict anatomical solar ultraviolet exposure. In SAI Computing Conference (SAI) IEEE, 2016, 1344-1348. Proceedings of SAI Computing Conference,London, UK, 13-17 July 2016.

13. Religi, A., L. Moccozet, D. Vernez, A. Milon, C. Backes, J.L. Bulliard and L. Vuilleumier (2016) Prediction of anatomical exposure to solar UV: A case study for the head using SimUVEx v2. In e-Health Networking, Applications and Services (Healthcom), 1-6. Proceedings of 2016 IEEE 18th International Conference, Munich, Germany, 14-17 September 2016.

14. Kiss, B., B. Balázs, and G. Szijart (2004) VR-based Therapy. Medicine Meets Virtual Reality 12: Building a Better You: the Next Tools for Medical Education, Diagnosis, and Care (Vol. 98). IOS Press, US.

15. Chapman, S., and L. Bracegirdle (2007) Virtual human interaction system, U.S. Patent Application No. 11/776,853.

16. Fischl, B., L. Arthur, and M. D. Anders M. D. (2001) Automated manifold surgery: constructing geometrically accurate and topologically correct models of the human cerebral cortex. IEEE transactions on medical imaging 20.1: 70-80.

17. Volz, A., R. Blum, S. Häberling, and K. Khakzar (2007) Automatic, body measurements based generation of individual avatars using highly adjustable linear transformation. Digital Human Modeling, 453-459.

18. Honglun, H., S. Sun, and Y. Pan (2007) Research on virtual human in ergonomic simulation. Computers & Industrial Engineering 53.2, 350-356.

19. Ratner P. (2012) 3-D human modeling and animation. John Wiley & Sons Inc., Hoboken, New Jersey.

20. Abdel-Malek, K. (2007) Human modeling and applications special issue, Human Modeling and Applications Computer-Aided Design Volume 39, Special Issue 7, 539.

21. Aggarwal, J. K., & Park, S. (2004) Human motion: Modeling and recognition of actions and interactions. In 3D Data Processing, Visualization and Transmission, 2004. 3DPVT 2004, 640-647. Proceedings of the 2nd International Symposium IEEE,

22. Kimlin, M. G., A.V. Parisi and N.D. Downs (2003) Human UVA exposures estimated from ambient UVA measurements. Photochemical & Photobiological Sciences 2.4, 365-369.

23. Hoeppe, P., A. Oppenrieder, C. Erianto, P. Koepke, J. Reuder, M. Seefeldner, and D. Nowak (2004) Visualization of UV exposure of the human body based on data from a scanning UV-measuring system. International journal of biometeorology, 49(1), 18-25.

24. Schrempf, M., Haluza, D., Simic, S., Riechelmann, S., Graw, K., and Seckmeyer, G. (2016) Is multidirectional UV exposure responsible for increasing melanoma prevalence with altitude? A hypothesis based on calculations with a 3D-human exposure model. International journal of environmental research and public health, 13(10), 961.

25. Streicher, J. J., W.C. Culverhouse, M. S. Dulberg and R.J.Fornaro (2004) Modeling the anatomical distribution of sunlight. Photochemistry and photobiology, 79(1), 40-47.

26. Kuchinke, C., and N. Manuel (2003) An anisotropy correction method for all-sky measurements of diffuse UV-B erythemal irradiance. Journal of Atmospheric and Oceanic Technology 20.11, 1523-1533.

27. Vernez, D., A. Milon, L. Francioli, J.L. Bulliard, L. Vuilleumier and L. Moccozet (2011) A numeric model to simulate solar individual ultraviolet exposure. Photochemistry and photobiology, 87(3), 721-728.

28. Backes, C., A. Religi, L. Moccozet, L. Vuilleumier, D. Vernez and J.L. Bulliard (2018) Facial exposure to ultraviolet radiation: Predicted sun protection effectiveness of various hat styles. Photodermatology, Photoimmunology & Photomedicine journal (In press, DOI: 10.1111/phpp.12388)

29. World Health Organization. Ultraviolet radiation and health. Available at: http://www.who.int/uv/uv_and_health/en/. Accessed on 06 March 2018

30. Seckmeyer, G., M. Schrempf, A. Wieczorek, S. Riechelmann, K. Graw, S. Seckmeyer and M. Zankl (2013) A novel method to calculate solar UV exposure relevant to vitamin D production in humans. Photochemistry and photobiology, 89(4), 974-983.

31. Chadyšiene, R., and A. Girgždys (2008) Ultraviolet radiation albedo of natural surfaces. Journal of environmental engineering and landscape management, 16(2), 83-88.

32. McGee, R., Williams S., Cox B., Elwood M, Bulliard J-L (1995) A community survey of sun exposure, sunburn and sun protection. The New Zealand medical journal; 108: 508-510.

33. Ackermann S, Vuadens A, Levi F, Bulliard JL (2016) Sun protective behaviour and sunburn prevalence in primary and secondary schoolchildren in western Switzerland. Swiss Med Wkly; 146: w14370.

34. Parsons, P. G., Neale, R., Wolski, P., Green, A. (1998) The shady side of solar protection. The Medical Journal of Australia, 168(7), 327-330.

35. McMichael, J. R., Veledar, E., Chen, S. C. (2013) UV radiation protection by handheld umbrellas. JAMA dermatology, 149(6), 757-758.

36. Vanos, J. K., McKercher, G. R., Naughton, K., Lochbaum, M. (2017) Schoolyard Shade and Sun Exposure: Assessment of Personal Monitoring During Children's Physical Activity. Photochemistry and photobiology, 93(4), 1123-1132.

37. Seckmeyer, G., Schrempf, M., Wieczorek, A., Riechelmann, S., Graw, K., Seckmeyer, S., and Zankl, M. (2013) A novel method to calculate solar UV exposure relevant to vitamin D production in humans. Photochemistry and photobiology, 89(4), 974-983.

38. Verdebout, J. (2010) Estimating natural UV personal exposure with radiative transfer calculations. Radiation protection dosimetry, 141(3), 275-282.

39. Pope, S. J., and Godar, D. E. (2010) Solar UV geometric conversion factors: horizontal plane to cylinder model. Photochemistry and photobiology, 86(2), 457-466.

FIGURE CAPTIONS

Figure 1. Total UV exposure per minute received beneath shade structures during a full clear sky day (8AM - 5PM) as function of SZA for different anatomical zones (arm left, leg left, head and trunk).

Figure 2. Predictive Protection Factors (PPF [%]) as function of the hour for different anatomical zones (arm left, leg left, head and trunk). Each PPF was calculated considering total erythemal UV radiation for a whole hour.

Figure 3. Direct, diffuse and reflected exposure during a clear sky summer day (17/07/2014) for shade structure 1 (a), shade structure 2 (b) and shade structure 3 (c), considering the head and trunk.

Figure 4. 3D rendering for fixed simulations from 12PM to 2PM (17/07/2014) for a male mannequin with a) small/low shade structure, b) small/high shade structure, c) large/high shade structure. In the small frame the morphologies of the male mannequin for the three shade structures are displayed. The different colors refer to different anatomical subzones.

TABLES

Table 1. Predictive protection factor (PPF, in %) of three shade structures for main anatomical regions between 12 PM and 2 PM.

		Without protection			**Shade Structure 1**			**Shade structure 2**			**Shade structure 3**		
		Diffuse	Direct	Reflected	Diffuse	Direct	Reflected	Diffuse	Direct	Reflected	Diffuse	Direct	Reflected
Head	PPF %	-	-	-	44.4	99.9	3.3	29.1	99.9	3.2	55.8	99.9	3.1
	Dose (J/m^2)	323.6	224.9	5.4	180.1	0.1	5.3	229.5	0.1	5.3	143.1	0.1	5.2
Neck	PPF %	-	-	-	25.4	100	8.9	16.7	97.1	8.9	39.7	99.9	8.9
	Dose (J/m^2)	304.7	195.1	5.9	227.1	0	5.3	253.5	5.6	5.3	183.2	0.2	5.3
Arm Left	PPF %		-	-	22.9	69.3	8.2	18.9	55.8	7.9	38.9	99.9	7.7
	Dose (J/m^2)	260.9	180.2	5.8	200.9	55.3	4.8	211.5	79.6	4.8	159.4	0.1	4.8
Arm Right	PPF %	-	-	-	22.3	33.6	8.1	18.5	20.5	7.7	38.1	99.9	7.5
	Dose (J/m^2)	263.3	227.8	5.3	204.5	151.2	4.8	214.7	181.2	4.8	162.9	0.1	4.9
Trunk	PPF %	-	-	-	26.1	83.3	14	21.9	60.5	13.8	37.5	99.9	13.6
	Dose (J/m^2)	260.7	174.4	6.7	192.7	28.2	5.8	203.7	68.9	5.8	162.9	0.17	5.8
Leg Left	PPF %	-	-	-	20.3	4.4	11.4	18.7	3.9	11.2	28.9	69.1	11
	Dose (J/m^2)	252.4	194.7	6.4	201.3	186.1	5.7	205.3	187.2	5.7	179.3	60.1	5.7
Leg Right	PPF %	-	-	-	21.7	18.7	12.9	19.9	18.5	12.7	30.9	68.1	12.5
	Dose (J/m^2)	253.7	213.1	6.4	198.6	173.2	5.5	203.1	173.7	5.6	175.2	67.9	5.6

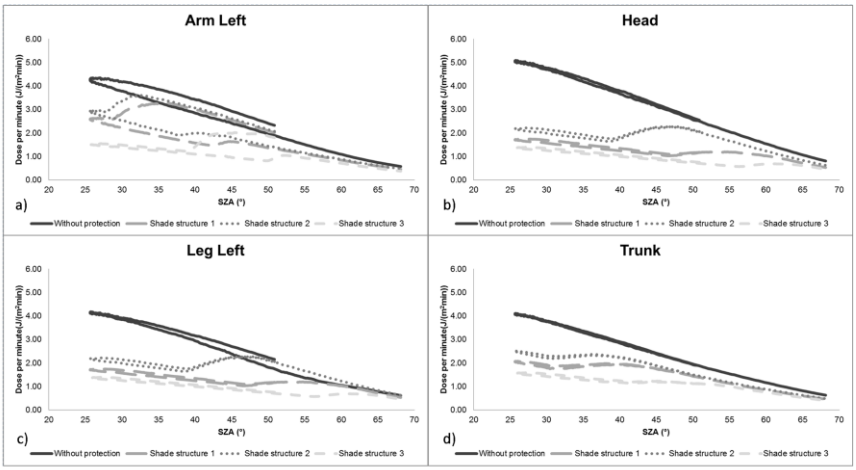
Arm Left
Dose per minute (J/(m²min))
SZA (°)
a)
Without protection
Shade structure 1
Shade structure 2
Shade structure 3
Head
b)
Leg Left
c)
Trunk
d)

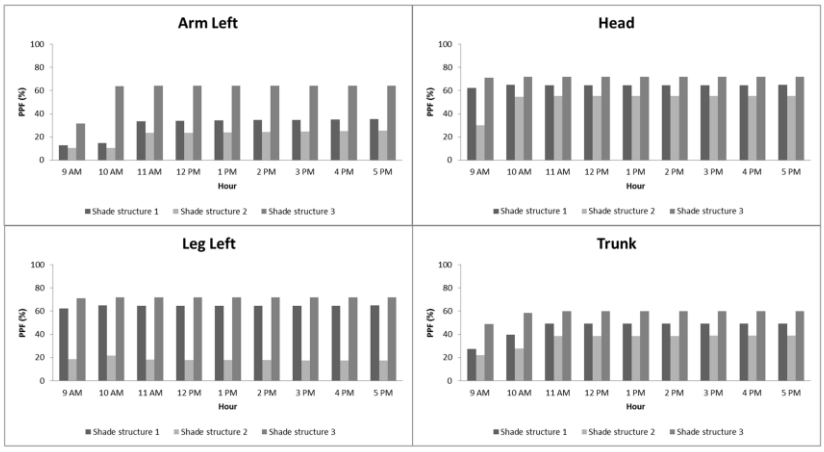
Arm Left
PPF (%)
100
80
60
40
20
0
9 AM
10 AM
11 AM
12 PM
1 PM
2 PM
3 PM
4 PM
5 PM
Hour
Shade structure 1
Shade structure 2
Shade structure 3

Head
PPF (%)
100
80
60
40
20
0
9 AM
10 AM
11 AM
12 PM
1 PM
2 PM
3 PM
4 PM
5 PM
Hour
Shade structure 1
Shade structure 2
Shade structure 3

Leg Left
PPF (%)
100
80
60
40
20
0
9 AM
10 AM
11 AM
12 PM
1 PM
2 PM
3 PM
4 PM
5 PM
Hour
Shade structure 1
Shade structure 2
Shade structure 3

Trunk
PPF (%)
100
80
60
40
20
0
9 AM
10 AM
11 AM
12 PM
1 PM
2 PM
3 PM
4 PM
5 PM
Hour
Shade structure 1
Shade structure 2
Shade structure 3

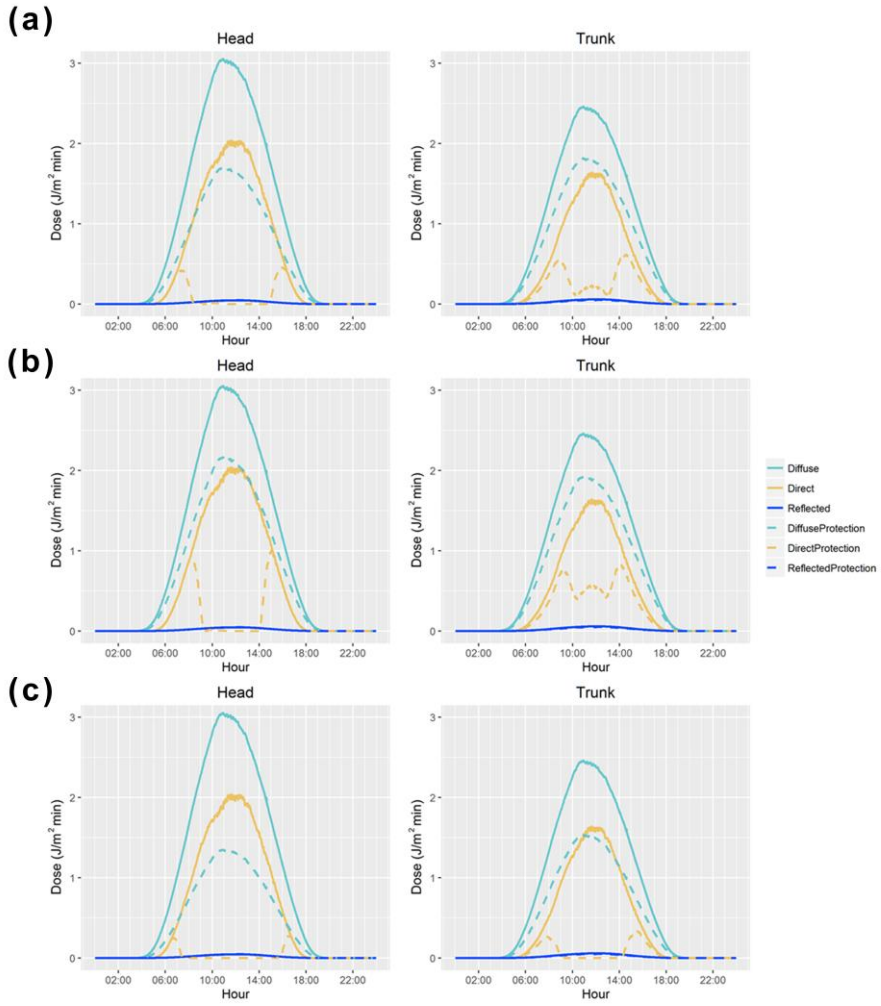
(a)
Head
Trunk
(b)
Head
Trunk
(c)
Head
Trunk
Dose (J/m² min)
Hour
02:00
06:00
10:00
14:00
18:00
22:00
0
1
2
3
Diffuse
Direct
Reflected
DiffuseProtection
DirectProtection
ReflectedProtection

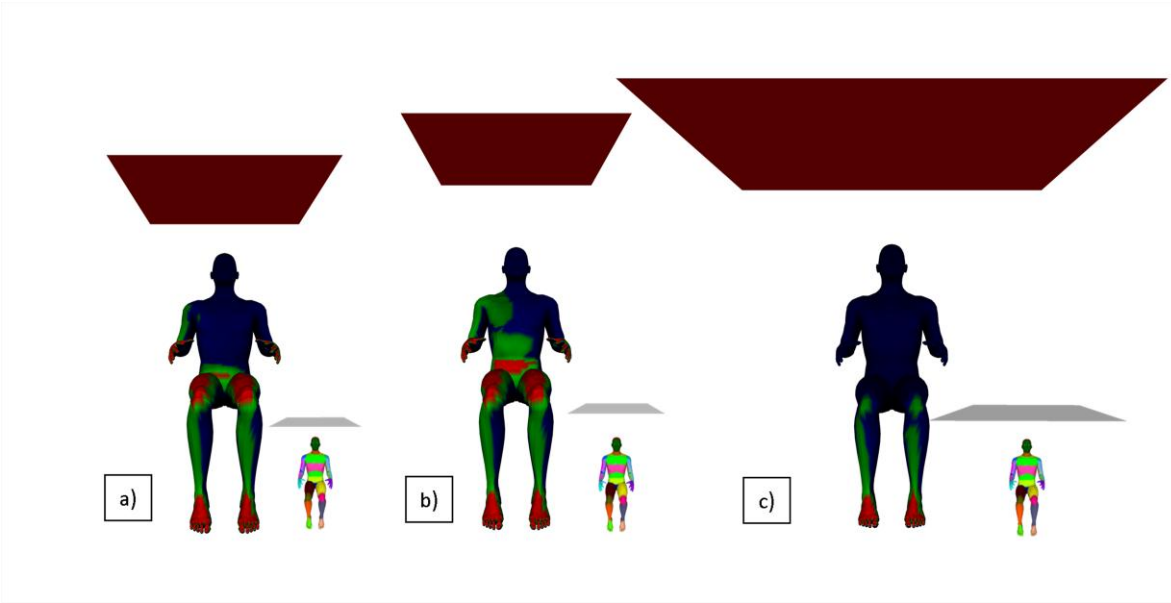
a)
b)
c)